Tracer gas techniques for airflow characterization in double skin facades

Building and Environment 212 (2022) 108803

Contents lists available at ScienceDirect

Building and Environment

journal homepage: www.elsevier.com/locate/buildenv

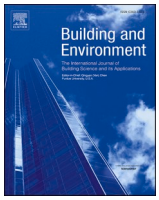

Tracer gas techniques for airflow characterization in double skin facades

Aleksandar Jankovic [a], Giovanni Gennaro [b], Gaurav Chaudhary [a], Francesco Goia [a,*], Fabio Favoino [b]

[a] Department of Architecture and Technology, Norwegian University of Science and Technology, NTNU, Trondheim, Norway
[b] Department of Energy, Politecnico di Torino, Italy

ARTICLE INFO

Keywords:
Tracer gas techniques
Constant injection methods
Decay method
Velocity traverse method
Double-skin facade
Experiment
Airflow characterization

ABSTRACT

Monitoring airflow rates and fluid dynamics phenomena in the ventilated cavity is a challenging aspect of the experimental assessment of the performance of double-skin facades (DSF). There are various methods to characterize the fluid-dynamics behavior of DSF, but each of these has its advantages and drawbacks. This paper presents the airflow characterization in the cavity of a double-skin façade installed in a full-scale outdoor facility through various methods, and, more specifically, it compares two tracer gas methods with the velocity traverse method. In the paper, we highlight how different characterization results can be explained by considering the features of each method, and how these differences are linked to velocity ranges and airflows in the cavity. By discussing (i) the challenges of these methods and their applicability, (ii) the requirements in terms of experimental set-up and (iii) the limitations linked to instrumentation, we aim to enhance the discussion on experimental methods for advanced building envelope characterization and contribute to a more grounded understanding of the suitability of tracer gas methods for in-field characterization of airflows in facades.

1. Introduction

1.1. Background

Increasing the performance of building envelope systems is a long-established trend in research that aims at developing building skins that minimize energy use and maximize user comfort across different domains. This has lead to a large range of concepts and technologies in recent years [1] that are transforming the building envelope from being a problematic component of the construction to being an interesting locus of possibilities. Advanced concepts and technologies that consider the building envelope not as static but as a dynamic, active system have been developed within this research and development avenue [2]. Such an envelope should act as a living membrane that continuously changes its interactions with the indoor and outdoor environment by filtering mass and energy fluxes [3]. The most advanced dynamic building envelope components are responsive [4] and adaptive [2] building skins, and double skin facades (DSF) are a well-established concept in both research and industrial development that makes highly transparent skins highly efficient [5]. In simple terms, a DSF is a multi-layered glazed structure with an external and internal layer (the skins) and a buffer space in between (usually ventilated in different ways) that can host a solar shading device to enable continuous control of solar loads [6]. This envelope system allows a high degree of flexibility in managing the incoming thermal and visual loads, it can support the pre-heating of ventilation air, and in the most general terms, it can be operated as a dynamic interface between the outdoor and the indoor space [7]. A fully glazed facade brings the transparency often desired by architects when designing a residential or commercial building [8]. In addition, it enables balancing visual comfort, visual attractiveness, sound insulation, thermal comfort and energy savings [9]. However, DSFs are more expensive than traditional single-layer façades, and if they are not well designed and operated, the marginally increased performance is hardly able to justify their costs, or in the worst scenarios they could present a lower performance than conventional envelopes [10].

Even though the DSF is a long-established concept with many applications in real buildings, there is still much research ongoing focusing on both the optimization of the system in terms of construction features and the optimization of the control strategies and algorithms to manage the dynamic operation of DSFs dynamically operated. In this latter topic, the management of shading devices [11,12] and of the airflow in the ventilated cavity, and the interactions between these two elements interact [13,14] are key topics to ensure optimal performance of DSF. A deep understanding of how DSFs can be efficiently designed and managed depends on how well the physical processes occurring in the

* Corresponding author.
E-mail address: francesco.goia@ntnu.no (F. Goia).

https://doi.org/10.1016/j.buildenv.2022.108803
Received 30 September 2021; Received in revised form 11 January 2022; Accepted 15 January 2022
Available online 21 January 2022

Nomenclature

Acronyms

CCM	Constant concentration method
CIM	Constant injection method
CMOS	Complementary metal-oxide-semiconductor
DM	Decay method
DVM	Direct velocity measurements
DSF	Double-skin facade
HVAC	Heating and ventilation air conditioning
LDV	Laser doppler velocimetry
PIV	Particle image velocimetry
USV	Ultrasound velocimetry
VPM	Velocity profile method
VTM	Velocity traverse method

Symbols

C	Concentration [ppm]
p	p-value [−]
t	time [s]
V	Volume [m^3]
V	Airflow rate [m^3s^{-1}]

Subscripts

b	Background
c	Cavity
tg	Tracer gas

DSF are understood and predicted. The most reliable insight is offered by experimental investigations [15], and many authors have performed experiments with different levels of complexity ranging from natural experiments [16–18] to those controlled with only thermal [19,20] or wind environment [21] to the experiments performed in both controlled thermal and radiative environment [15,22–24]. Data from experimental activities can also validate numerical models [25], opening up a path for design- and control optimization based on simulation.

The experimental characterization and performance assessment of a double skin façade (DSF) is a complex task, and well-established methods suitable for conventional envelope systems are often not capable of capturing the overall performance and measuring particular phenomena occurring in a DSF [26]. One of the most complex parts, if not the most complex one, concerns the determination of the airflow in the cavity, and this task is especially challenging when only naturally induced forces drive the airflow in the cavity. Various methods and techniques have been commonly adopted to monitor airflow rate, and many are standardized for the airflow estimation in HVAC ducts [27]. At the same time, there are no clearly defined procedures for measuring DSF cavities, which are environments characterized by a higher degree of inhomogeneity compared to HVAC ducts. The methods for airflow assessment differ in the complexity and cost of the experimental set-up, accuracy, amount of information they can offer and applicability for in situ measurements. For some techniques, such as direct velocimetry, recommendations exist for more reliable set-ups that reduce the experimental error. While direct velocimetry is quite well known, and there is a clear understanding of how much this technique can offer, other methods need further research to evaluate their accuracy and applicability for airflow measurements in DSFs.

1.2. Research aims, objectives, and paper structure

In this paper, we present the results of a set of experimental measurements obtained to assess and compare different techniques for airflow estimation. This investigation is based on a multi-day experimental campaign of the DSF hosted in a full-scale outdoor test facility. Two gas tracer techniques, more precisely the so-called *decay method* (DM) and *constant injection method* (CIM), were tested and compared with the velocity traverse method (VTM), a well-established (and relatively simple) technique to measure the total airflow in a duct section. Both of the gas tracer techniques analyses in this paper are state-of-the-art methods that have been successfully applied for airflow measurements in HVAC systems with forced ventilation [28–30] or infiltration/exfiltration assessment in rooms and larger volumes [31,32]. However, there is almost no research that deals with the application of gas tracer techniques for measuring airflow in DSFs, other than investigations [18,26,33,34] that employ only a constant injection method. Among these, only the research of Kalyanova [26] investigates the applicability of the constant injection method in DSFs and compares it with other more common methods. Intending to expand knowledge about this technique and the decay method, which has not yet been employed in DSF, this research aims to identify challenges and issues related to the different experimental set-ups and measurement procedures applied to double-skin facades in actual conditions.

To do this, the methodological steps that we adopted were: to instrument (as described in more detail in the next section of the paper) a full-scale mock-up of a DSF installed on an outdoor test facility; to run several rounds of measurements with different techniques over a specific range of (assumed) airflows, and varying some controllable variables; to apply statistical analysis techniques to understand the relevance and the role of controllable and uncontrollable variables.

The experiments and the results presented in the paper give insights on: (i) how to perform the two gas tracer techniques, (ii) why they may lead to different results, as well as (iii) how the outcomes of these methods compare to the estimation of the airflow through hot-wire anemometry. Finally, it would be possible to suggest that one method may better suit a specific situation and airflow ranges in the cavity, though there are some uncertainties and limitations in the study primarily linked to the complexity of measuring a highly transient phenomenon in an in-field like installation. Aside from the measurement that resulted from the tests, which allowed us to characterize the tested façade, the outcomes of this research can be of interest to researchers who want to apply gas tracer techniques. Moreover, our research contribute to the development of standardized procedures for setting up the correct experimental set-up and carrying out measurements with the highest possible confidence.

In the following sections of the paper, we will: classify and review existing experimental techniques for airflow characterization in DSFs (Section 2); describe in detail the experimental set-up and methodology, focusing on DSF mock-up specifications, characteristics of the measurement equipment and details about the experimental design and procedures (Section 3); present the results and the comparison between gas tracer techniquesand VTM, along with the details on correlation analysis, discuss the challenges and possibilities of these methods, and argue which methods are suitable for airflow characterization in different situations (Section 4); draw conclusive remarks of our study (Section 5).

2. Experimental techniques for airflow characterization

Experimental investigation of airflow varies by complexity and the depth of the insight it offers, and, generally, it can be divided into three categories/groups: bulk airflow measurements, direct velocity measurements (DVM) and non-intrusive velocity measurements methods, such as ultrasound measurement of velocity (USV), particle image (PIV) or laser doppler velocimetry (LDV) [35]. A short introduction to these three families of available methods is provided for the sake of completeness even if, as previously mentioned, we will focus in this paper on bulk airflow measurements through tracer gas and on direct velocity measurements, and we will not explore other techniques because of some intrinsic limitation they present for in-field application.

In particular, the last two categories (PIV and LDV) can provide turbulent quantity analysis, offering a large amount of information about the flow, but at the same time, they are very complex to realize in terms of the experimental design and sensitivity [36] and are almost entirely limited to laboratory environments, while their in-field application is almost inoperable and difficult to carry out.

2.1. Direct velocity measurements

A method that uses the direct velocity measurements acquired by hot-wire, hot-sphere or vane anemometers represents the most applied method for airflow estimation in DSF, especially when it comes to in-field measurements. The experimental set-up may vary in complexity and in the amount of information it can offer, from the most basic one, where only one anemometer is used, to the most advanced such as the velocity profile method (VPM) [8,21,22,33,37]. In a VPM, several anemometers are placed along one or more heights inside the cavity, indicating in such a way the spatial distribution of the airflow. Spatial discretisation of such information needs to be balanced with the measurement accuracy since the sensors' probes, cable, and physical support represent obstacles to the flow. Besides the reduced flexibility of the experimental set-up, the main disadvantages of this method are the limited amount of information about the spatial structure of the flow provided by the punctual measurements, the issues with the determination of the airflow direction [38] and the inadequate accuracy for the lowest velocity ranges. Regardless of these limitations, studies have shown that this technique offers the best balance between complexity, set-up cost, accuracy, amount of provided information and applicability in in-field conditions.

2.2. Non-intrusive techniques

Non-intrusive techniques, such as laser Doppler (LDV), particle image (PIV) and ultrasound (USV) velocimetry, employ optical/acoustics methods for the determination of the airflow in the cavity. LDV assesses the velocity in fluid flow in a non-intrusive way by recording the Doppler (frequency) shift between emitted and reflected laser beams. The PIV technique obtains instantaneous velocity fields by recording images of particles at successive times, the velocity of the fluid is determined by the characteristics of the light scattered from fine particles illuminated by monochromatic light. USV is based on either measuring frequency shift or the difference in the transit time between two oppositely emitted ultrasonic pulses. USV techniques show the promising possibility for long-term airflow monitoring in DSFs, but further research is needed to fully understand their applicability [31], especially in relation to the range of velocity that can be accurately measured by USV sensors. Many non-intrusive techniques such as those based on LDV and PIV are characterized by excellent accuracy, but they are at the same time limited by laboratory-restricted instrumentation, cost, complexity and sensitivity of the experimental set-up [36,39,40], therefore their application for in-field continuous measurements in buildings is unfeasible.

2.3. Bulk airflow method

Bulk airflow methods are based either on measuring the pressure difference along the airflow path in a DSF cavity (pressure difference method) or on monitoring the concentration of a tracer gas inside the cavity (trace gas techniques) [41]. The first method needs calibration, usually performed in the laboratory, to determine the empirical relation between the airflow rate and the measured pressure difference. Once it is calibrated, then it is relatively easy to set up the experiment in field settings. Still, care should be taken when choosing the representative sampling point for external pressure since it is susceptible to wind-induced turbulence [37]. The method shows excellent accuracy in estimating the mechanical flow in laboratory conditions, yet further research is needed to assess its applicability for real (dynamical) environments and naturally ventilated DSFs.

Tracer gas techniques are well-known methods to measure airflow rate in rooms and larger volumes. The following tracer gas techniques are the most commonly adopted: constant injection (CIM), constant concentration (CCM) and the decay method (DM). Sulfur hexafluoride (SF_6) or carbon dioxide (CO_2) are often used as a tracer gas, with the latter used more often as a preferred marker due to its low cost, faster response of CO_2 sensors and being a less harmful greenhouse gas with 23,500 times lower global warming potential (GWP) than SF_6 [42]. In DM, a particular concentration is achieved at the beginning of the experiment $C\ (t_1)$, whereafter the time $(t_2\text{-}t_1)$ required for the tracer gas to descend close to the background reference level $C\ (t_2)$ is measured [43], based on which the average airflow rate $\bar{\dot{V}}$ is assessed:

$$\bar{\dot{V}} = \frac{V}{t_2 - t_1}\log_e\frac{C(t_1)}{C(t_2)} \tag{1}$$

where V represent volume of DSF cavity.

In a CIM, a fixed and known amount of tracer gas V_{tg} is steadily injected while the fluctuating concentration $C_c\ (t)$ is measured downstream so one can estimate the airflow rate $q\ (t)$ [29]:

$$\dot{V}(t) = 10^6\frac{\dot{V}_{tg}}{C_c(t) - C_b} \tag{2}$$

Background concentration C_b needs to be assessed as well, and if it is expressed in *ppm*, then a coefficient 10^6 *ppm* should be used in the equation. In a CCM, instead of injecting a fixed amount of tracer gas, a variable quantity is infused V_{tg} (t) so that constant concentration C_c is achieved downstream or in the volume where the measurement is carried out [44]:

$$\dot{V}(t) = 10^6\frac{\dot{V}_{tg}(t)}{C_c - C_b} \tag{3}$$

In their review, Remion and colleagues [45] concluded that the gas tracer techniques do not interfere with the flow and that they better account for infiltration/exfiltration flows compared to conventional airflow measurement methods [46]. However, if not met, some limiting requirements, such as the assumption of gas tracer homogeneity and the flow steadiness during measurements, lead to increased uncertainties [47]. In addition, tracer gas techniques are intended for short-time characterization, and they are not suitable for continuous monitoring. Applications are primarily seen in ducts (with forced ventilation) and not commonly in DSF cavities [21,22]. Therefore, there are no clear guidelines on the experimental set-up, such as the preferred position and the number of emission and sampling points in the DSF cavity [47]. Furthermore, the assumption of non-interfering with the flow/driving forces is questionable as the tubes releasing gas and sensors measuring concentration need to be inserted into the duct/cavity. As such, they represent obstruction to the flow when the cavity is not very large realtive to the space occupied by the experimental set-up. Other sources of inaccuracies, such as drainage of emitted tracer gas near the opening, can result in too high airflow rates [41]. Also, injection of a significant amount of tracer gas could affect the fluid dynamics in the duct/cavity since the CO_2 or SF_6 have different gas properties than air [48].

3. Experimental set-up and methodology

3.1. Experimental test-rig

We performed the airflow characterization presented in this paper using a full-scale mock-up of a DSF installed in the outdoor test TWINS test facility [49]. The test facility has dimensions of (3.5 m (l) x 1.6 m (w) x 3 m (h)), and for this experimental campaign it hosted a DSF of (1.5 m (w) x 2.8 m (h)) which consised of 2 skins, made up of 2 double glazing units (1.22 m × 2.0 m, U-value = 1.2 W/m^{2}K, g-value = 0.47),

separated by an air cavity (250 mm) (Fig. 1). The DSF was oriented nearly perfectly toward the south. It had four axial vertical fans (maximum flow of 220 m^3/h each) placed at 2.6 m from the bottom, though only a small fraction of the maximum theoretical flow rate can be achieved under real operative conditions. The cavity hosted a roller blind to control solar gain. Different airflow paths between outdoor and indoor environments could be tested by operating the vents (1.5 m × 0.3 m).

The DSF module was equipped with the following sensors used for the airflow characterization: four air velocity and temperature transducers at two different heights inside the cavity (1 and 2 m height from the bottom of the cavity), five CO_2 concentration sensors (based on CMOS technology) that were previously calibrated in the laboratory against a gas tracer analyzer and could also measure temperature and relative humidity, and the outdoor anemometer to monitor both wind speed and direction in the horizontal plane (Fig. 1). Hot-wire anemometers could measure air velocity in four different ranges, but according to prevailing measurement conditions, we opted for the lowest output range (0.05 ~ 1 m/s) with the instrumental error of ±(0.1 m/s + 3%). The outdoor anemometer was located left of the DSF (Fig. 1). One CO_2 sensor was placed outside the DSF to measure the background CO_2 level and four were distributed in the cavity. The measurement sampling rate was 20 s (coherent with the CO_2 response time of the sensor) and CO_2 concentration was kept within the range of values read by the sensor. The following set-up was built to supply the CO_2 inside the cavity: a CO_2 tank equipped with a valve was placed outside the test facility; an asameter was located downstream of the tank and a gas flow meter was used to measure and control the injected CO_2 flow (Fig. 1).

3.2. Experimental procedures

For the CIM, a constant CO_2 flow was injected at the bottom of the cavity (8 pipes near the inlet vents). The CO_2 sensors were located in the upper part of the cavity to measure the CO_2 concentration at the exhaust. The control valve regulated the amount of the injected CO_2, which depended on the configuration. It was necessary to intensify the volumetric flow of injected CO_2 with the enhancement of the fan speed and DSF openings (Fig. 2) in order to keep a large enough difference between the background CO_2 concentration and the CO_2 concentration in the cavity. However, there was a slight increase in average CO_2 level in the cavity as configurations shifted from left to right, as shown in Fig. 2.

In the DM, four source pipes were set per side at two different heights and the CO_2 sensors were placed near the air velocity transmitters (Fig. 3). The CO_2 was injected at different cavity heights to reach the target CO_2 concentration (with all vents closed) and bottom fans were installed and used to ensure the perfect mixing of the CO_2 in the cavity (Fig. 1 right). When the target CO_2 concentration was reached, the bottom fans were switched off and the vents and top (main) fans were operated according to the tested configuration. Then, the time required for the CO_2 concentration to drop close to the background level was measured. It was necessary to inject higher volumes of CO_2 for configurations with larger openings to maintain a sufficient decay time in order to ensure a robust measurement. For example, the starting concentration needed to be between 20,000 and 25,000 ppm for the configurations with large openings (100%) to have a decay time of at least *100 s* (Fig. 3). However, as described in more detail in the next section, such a large CO_2 amount in the cavity affected the air mixture and may have changed its dynamics. As the volume of injected CO_2 normalized per volume of DSF cavity increased, the difference between it and the average concentration in the cavity increased too, meaning that one part was either directly lost to the outside or descended to the lower parts of the cavity below the level of the sensors.

An attempt was made to minimize the influence of sudden changes of external factors by placing a black textile screen in front of the DSF and keeping the facility's door open. The screen was hung parallel to the outer surface of DSF at a distance of around 40 cm from the surface. The textile screen was also placed in front of both openings, shielding them from the direct effect of the wind. Here, it is important to highlight that due to the geometry of the openings (each realized by means of a top-hang, outward opening sash - see the schematic representation in Fig. 3), the presence of the screen did not obstruct the flow through the openings, but only shielded them from direct wind strikes. The black textile screen protected the DSF during both CIM and DM measurements.

Consequently, the wind influence was reduced to a certain extent, and the thermal gradient was kept to a minimal level compared to conditions one may experience in a DSF under real operations. Temperature differences between indoor (inside the test cell) and outdoor ranged between 5.0 and 7.4 °C, with an average value of 5.9 °C during CIM and 6.4 °C during DM measurements. The solar irradiance on the DSF's vertical surface ranged between 0 and 30.4 Wm^{-2}, with an average value of around 3 Wm^{-2} during CIM and 16 Wm^{-2} during DM measurements. Our goal in implementing these settings was to make the flow in the cavity as homogeneous and steady-state as possible by making it driven by the fan to the largest extent. By completely controlling boundary conditions, we could eliminate sudden and abrupt changes in

Fig. 1. An experimental set-up consisting of CO_2-supply instrumentation, the DSF test sample, the automatic weather station (left) and the view from the inside of the cell (right).

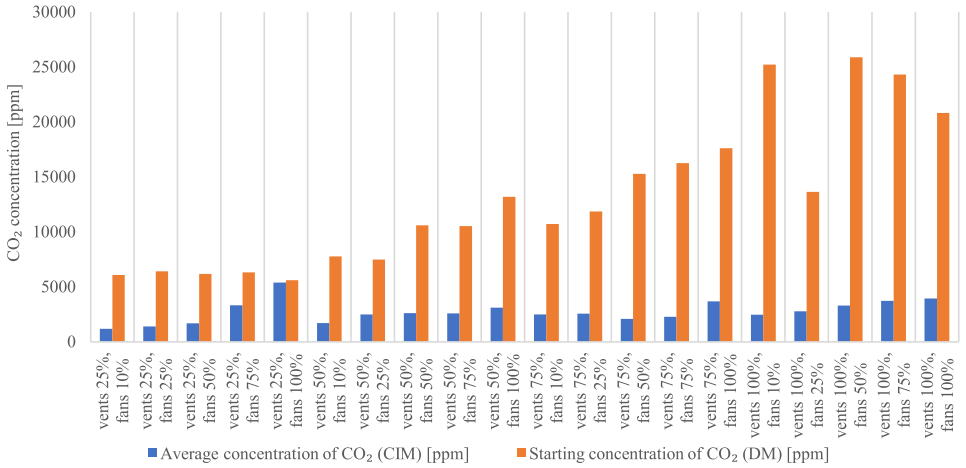

Fig. 2. The starting and the average CO_2 concentration in the cavity.

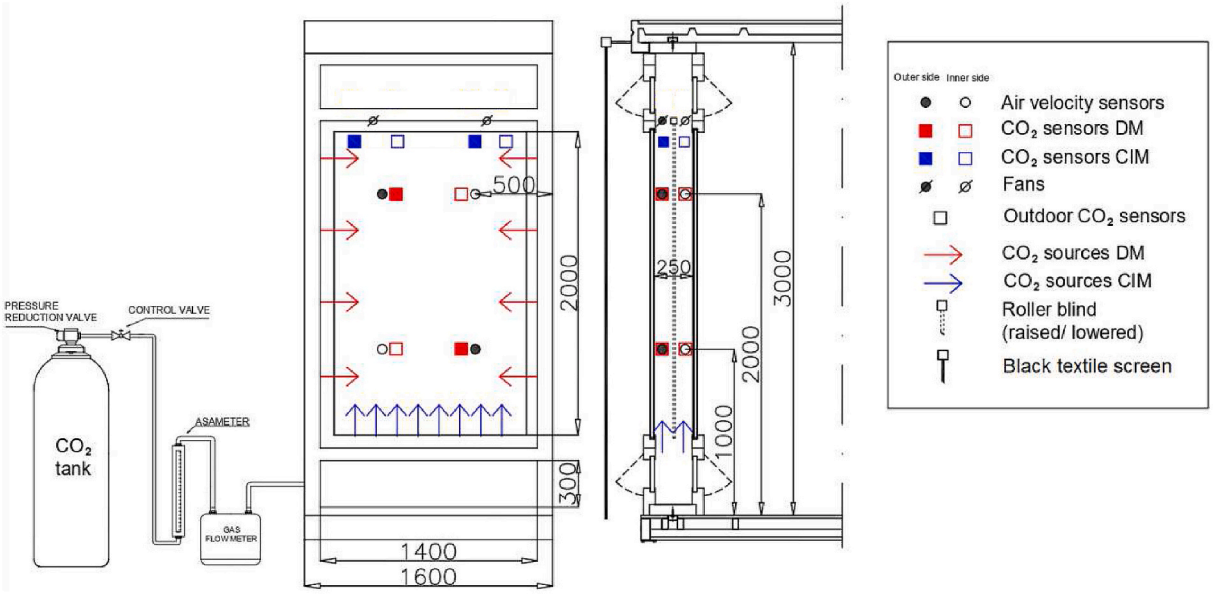

Fig. 3. Schematic representation of experimental set-up for different airflow characterization methods.

external factors that may undermine the assumption of homogeneity and steady-state conditions in the cavity. Therefore, one of the assumptions underpinning this study was that the velocity profile was symmetrical and directed upward, which allowed us to calculate the airflow rate using the velocity traverse method (VTM) more easily.

The airflow rate was calculated in three ways by multiplying the cross-sectional area of the cavity and the average velocity (obtained from two sensors) for the corresponding height. The first two ways involved correction of measured velocity by the factor k [27,50], while the third assumed that measured velocity corresponded to average velocity in the cavity. Comparing three approaches with the high-precise airflow measurements of the ultrasonic flow meter in the laboratory showed us that the third approach was most suitable for the airflow calculation in the specified conditions [54]. EN ISO 12569:2012 [31] and EN 12599:2012 [28] provided the basis for calculating the airflow for the DM and the CIM, respectively.

Different DSF cavity configurations were tested multiple times, comparing DM and CIM bulk airflow estimations with airflow assessment via the VTM. Twenty-three different configurations of DSF were tested with both DM and CIM by varying vent opening (25, 50, 75 and 100%), fan speeds (10, 25, 50, 75, and 100%) and roller blind's position (displaced and retracted). Only one airflow path was investigated in this experimental study for both the CIM and DM, i.e., the outdoor air curtain mode. In this ventilation mode, the outdoor air enters the cavity, and when it leaves the cavity, it is released again towards the outdoor environment. The DSF is therefore isolated from the test cell's indoor air, and outdoor air cannot enter the indoor space behind the DSF by going through the DSF's cavity.

The sampling of all the different physical quantities was performed every 20 s, which was the declared time constant of the employed CO_2 concentration sensors, while the duration of each experimental run depended on the characteristics of the chosen method. In CIM, the data acquisition period of each measurement run was 3 min, while for the DM, the duration depended on the decay time, which was between 600 and 100 s.

4. Results and discussion

4.1. Airflow assessment analysis

Both DM and CIM were tested and compared to the VTM, with DM showing a larger offset than CIM. In two cases with the raised roller blind, the estimated airflow value obtained through CIM exceeded the range of combined instrumental and measurement uncertainty added to the value obtained by VTM (Fig. 4). In almost all cases (12 out of 15), the airflow was overestimated compared to VTM, with an average relative error of 52%. However, VTM can not be considered a benchmark for evaluating other methods for the lowest airflow range due to the large instrumental error (indicated with vertical error bars) and low threshold value (0.05 ms^{-1}) of velocity sensors. Alternatively, if we consider cases where VTM can be regarded as reliable (marked with blue and gray columns), the relative offset to VTM is 31%. Therefore, CIM can be considered relatively successful in airflow estimation for the average velocity range in the cavity of over 0.1 ms^{-1} (Fig. 7., dots over the black line). A positive correlation coefficient (0.71) between airflows obtained by the VTM and CIM confirmed the expected monotonic function between airflow and the opening size. As mentioned in experimental procedures, the injected CO_2 amount depended on the tested configuration. Experience in the experimental campaigns taught us that targeting levels below 2000 ppm can result in an unrealistic overestimation of the airflow or even in negative values because the CO_2 concentration in the cavity can get too close to or even fall below the background level. The upper limit of 5000 ppm proved to be high enough to prevent sudden drops to background levels, while at the same time low enough not to modify air mixture and dynamics.

DM and VTM showed a worse agreement. In nine cases, the assessment of DM was within the range of combined instrumental and measurement uncertainty of the VTM. The airflow derived by the VTM was considerably higher than obtained with DM (green bars in Fig. 5). However, due to the higher pressure drops caused by the small openings (25%) that led to lower airflow rates, velocity values below the instrumental threshold value were most likely present in those cases. Furthermore, considering the trend between VTM and openings in a reliable range (full colored bars in Fig. 5), it is probable that lower airflows than measured by VTM characterize smaller openings. Weighing the monotonic function between opening size and airflow assessed by DM, DM may be more suitable for low airflow assessment than VTM. As opposed to CIM, with an average relative error of 64%, the airflow in all cases by DM was underestimated compared to VTM. DM showed better agreement with VTM regarding monotonic function between airflow and size of the opening area and fans' speed (correlation coefficient between airflow values obtained by VTM and DM is 0.78).

For the case where the roller blind was lowered, both gas tracer techniques underestimated the airflow rate compared to the VTM, except CIM for the configuration with 75% opened vent and 100% turned on fans (Fig. 6). With an average relative error of 23%, CIM showed better agreement with VPM, while in the case of DM, the error is 51%. The general conclusion is that the estimation of the airflow rate via DM and CIM was more accurate when the roller blind is lowered than when it is not. One may think this originates from the tested configurations and the associated higher airflows, where there is generally better agreement between methods. However, it might be caused by the presence of the roller blind making the flow more structured in each half-cavity. For the cases with lowered roller blind, the airflow estimated by VTM was higher in the inner cavity than in the outer, which might be caused by the slightly higher inner glazing temperature that led to the accelerated upward motion in the inner cavity. In contrast, colder outer glazing reduced the flow in the outer cavity. A similar phenomenon can be seen with the DIM and CM methods, which indicate that gas tracer techniques can also provide hints about the airflow's spatial structure, although these techniques rely on the assumption of even distribution of the tracer gas particles in the measurement volume.

In both methods, it was noticed that measurements of certain CO_2 sensors deviated from the other. For example, in CIM, a CO_2 sensor installed at 2nd height in the inner cavity registered high fluctuations in CO_2 level, which led to the assessment of unrealistically extreme or even negative airflow rates. These fluctuations are most likely associated with sudden and sporadic direct penetrations of the wind (which has a lower CO_2 concentration), leading to violation of the good mixing assumption in the cavity. In DM, the decay curve for certain sensors showed different shapes and decay times, indicating non-uniform dispersion of injected CO_2 in the cavity. While one can think that differences in sensors' readings might be due to different devices being used, it is important to recall that all the sensors were calibrated in the laboratory before the experimental campaign. We can thus assume with a high degree of confidence that (substantially) different readings are meaningful and are not attributable to the sensor's performance difference. Therefore, care should be taken to select the sampling and injection point positions. It is recommended to use several sensors for measuring CO_2 concentration and to conduct run pretests to find the most suitable positions and eliminate discrepancies between measurements. Furthermore, the CO_2 injection points in the DM method need to be distributed evenly along

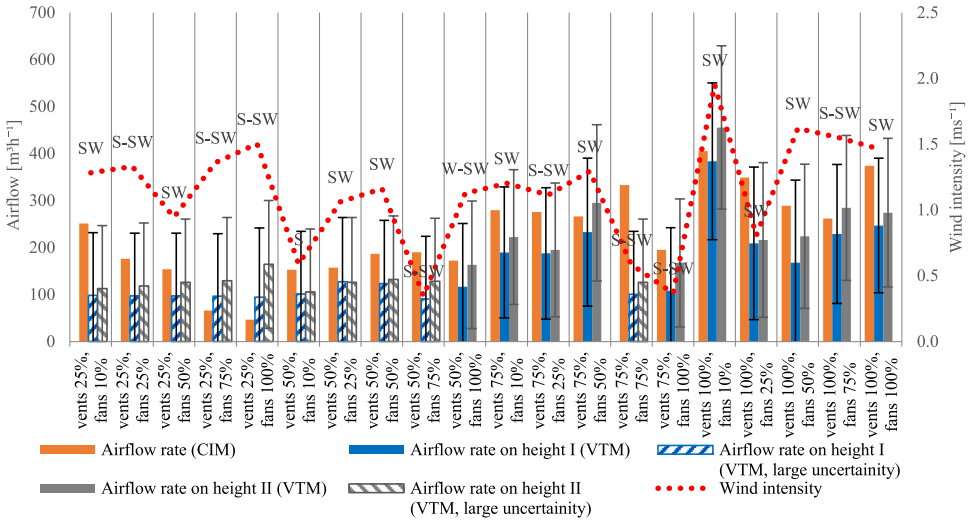

Fig. 4. Comparison of CIM and VTM for different tested configurations (raised roller blind).

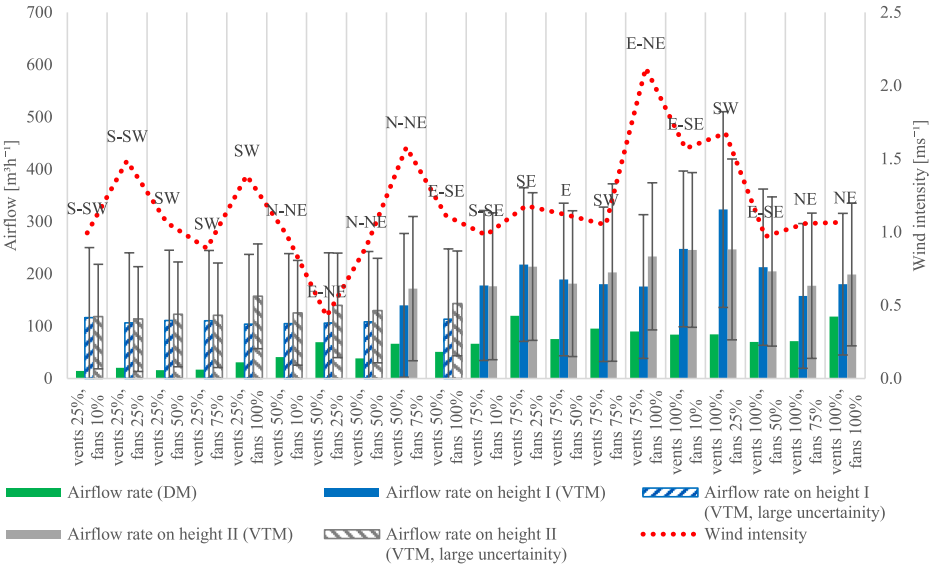

Fig. 5. Comparison of DM and VTM for different tested configurations (raised roller blind).

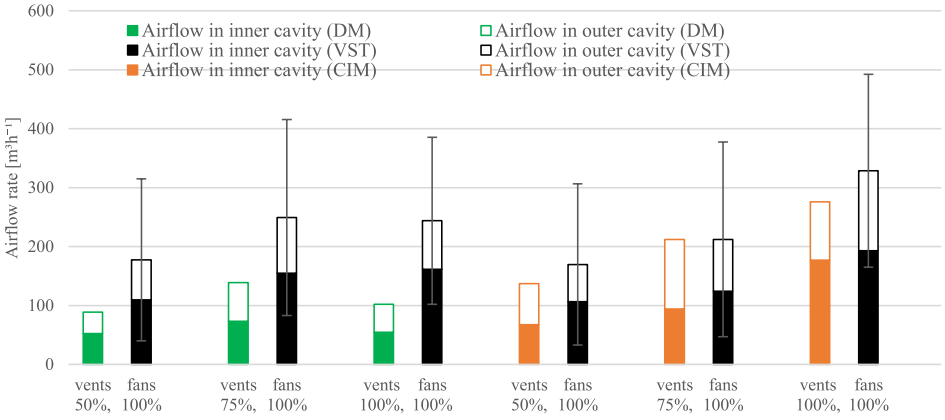

Fig. 6. Comparison of DM and CIM with VTM for different tested configurations (lowered roller blind).

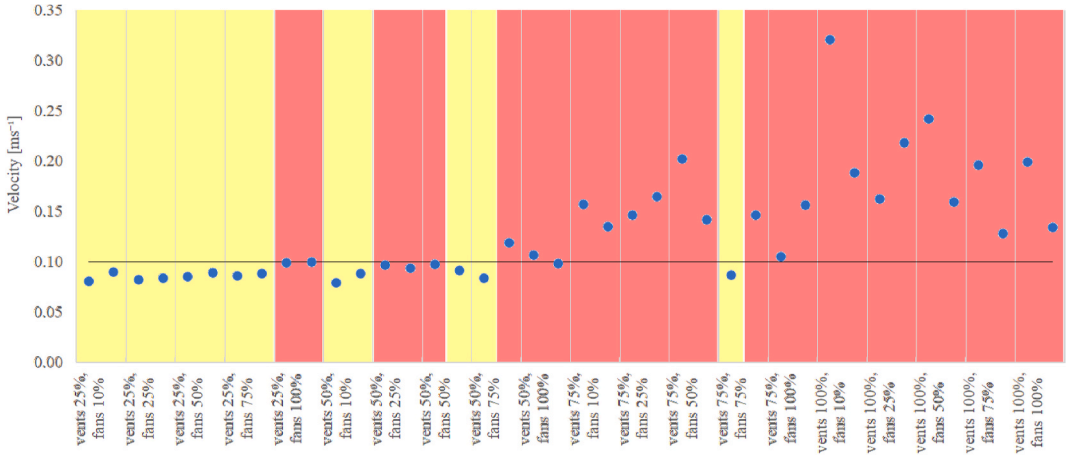

Fig. 7. Average velocity in the cavity and the assumed flow regime.

several heights to distribute CO_2 uniformly in the cavity.

4.2. Correlation analysis

To understand which factors influenced the airflow measurements and which controlled the airflow generation in the cavity, we ran a regression and correlation analysis using Pearson's correlation coefficient with a confidence level of 95% as a measure of dependence between variables. The results of the correlation analysis are shown in Table 1, and they refer to configurations with raised roller blinds. The temperature difference between the indoor and outdoor environment and the solar irradiance on the outer surface of the DSF were taken as factors that induce thermally buoyant flow, while the wind intensity and the opening size were taken as drivers of the wind-induced natural flow. Fans' speed was taken as an indicator of mechanical flow in the DSF cavity.

The results of correlation analysis showed that opening size and wind intensity had a positive correlation with airflow rates measured by all methods. That was especially true for the opening size, where a very strong/strong positive correlation was found with the airflow rates measured by all methods. VTM displayed a moderate/strong positive correlation between airflow rate and wind intensity, while CIM and DM saw there a weak positive correlation. Other quantities did not show such a directed dependence for all considered methods.

The regression analysis performance for airflows measured by VPM with velocities over 0.1 ms^{-1} showed that statistically significant factors ($p < 0.05$) in the generation of the airflow were the opening size ($p=0.008$) and the wind intensity ($p=0.006$). A regression model with the coefficient of determination of 0.71 excluded fan speed ($p=0.087$), temperature difference ($p=0.093$) and vertical solar irradiance ($p=0.926$) as statistically significant influencing factors. Based on both analyses, we can conclude that the airflow was to the greatest extent induced by the wind, where the opening, as expected, played a major role in controlling the rate. Also as expected, the correlation analysis showed that increasing the opening size and wind intensity lead to amplification of airflow. However, the influence of wind seems to have had a dominant role in controlling the flow rate even though dedicated expedients were implemented during the experiment to suppress the wind influence. This fact made it more complicated to ensure that the flow was homogeneous and under steady-state conditions. By setting the black textile screen, we may have significantly blocked the direct wind penetration in the cavity through the openings, especially for the smaller sizes (25 and 50%). However, it seemed that we could not completely eliminate associated turbulence and pressure field modifications caused by the wind. These caused air movement in and out the cavity, depending on wind intensity and direction. It was expected that the wind would increase pressure on the windward side of the test cell, while there would be a decrease on the leeward and lateral sides [51–53], with the addition that the presence of a black textile screen most likely reduced the influence of the wind from the clear southern direction. If we consider airflows assessed by VPM with velocities over 0.1 ms^{-1} on Figs. 4 and 5, it seems that winds with SW and S-SW directions amplified the airflow, while easterly winds suppressed the flow, which was in line with expectations [51–53]. However, due to the unknown wind's 3D behavior, along with instrumental limitations in measuring air speed values below 0.1 ms^{-1} and the complexity of weighing wind direction in statistical analysis, it was impossible to mathematically prove that wind direction amplified or hindered the airflow. Considering this, we can not claim that wind direction affected the measurements in a significant way, though it is very reasonable to assume that wind direction could have influenced the airflow in the cavity, even if its influence was probably not in the same range of magnitude as the wind intensity and the opening size. The wind is an uncontrollable variable in this type of experiment, and because of this feature, the only way to deal with it is to measure it as accurately as possible and to use statistical tools (in combination with repeated measurement runs) to infer its contribution.

Through the series of experimental settings adopted in the tests, we made the buoyant flow significantly low, especially for the medium and big size openings (75 and 100%). For these configurations, sudden wind strikes might have caused instabilities in the assumed "steady" state and oscillations in the CO_2 concentration, leading to airflow overestimation by CIM (the airflow estimated by this method is inversely proportional to the difference between CO_2 concentration in the cavity and the background level). Conversely, the decay time decreased with increasing airflow, which in turn depended on the vent opening percentage. To ensure sufficient decay time for larger openings (75 and 100%), high CO_2 concentration needed to be injected in the cavity (10,000–35,000 ppm), which might have caused its subsidence and resistance to upward air motion due to higher molar mass of CO_2.

Air velocities below and around the instrument threshold were most likely present in configurations with very small and some small openings (25 and 50%). Hot-wire anemometers determined these velocities with large uncertainty (Fig. 7, dots below black line). Consequently, we can assume that the correlation analysis related to VTM most likely did not outline the actual drivers and characteristics of the flow for these configurations. Here, the flow could be more driven by the thermal effects and the fan, and the correlation analysis related to the DM could characterize the flow better. Furthermore, we can assume that the DM can be a suitable measurement technique in cases with very low airflows (average velocity below 0.1 ms^{-1}). In those configurations (very small and small openings), the air behaves similarly and leaks slowly, just like in building spaces, where this method has found its successful application. However, more research and comparison with more precise measurement techniques, such as ultrasonic flow measurements, are needed to prove this.

The analysis of the measured velocities for the case with raised roller blind also revealed that flow was turbulent for almost all the configurations (Fig. 7, red area), except for the least opened vents (25%), where its nature cannot be judged due to too low velocities. Corresponding configurations where the flow could be laminar or transitional are indicated with yellow color in Fig. 7, while turbulent ones are marked red.

4.3. Limitations

Our study highlighted how some variables could be tricky to control regardless of the many efforts put in place to have the highest possible control over the experimental domain. In this context, statistical tools that can allocate the variance of the response variable to different factors represent a valuable technique for better process understanding and interpretation of data obtained from in-field experiments. Furthermore,

Table 1
Correlation analysis between airflow rates measured by different methods and various factors.

		Wind-induced natural flow		Mechanical flow	Thermally-induced natural flow	
		Wind intensity	Opening size	Fan speed	Temperature difference	Solar irradiance
Airflow rate	*VTM during CIM*	0.60	0.75	−0.16	−0.01	0.80
	VTM during DM	0.48	0.85	−0.09	0.10	−0.33
	CIM	0.19	0.82	−0.27	0.10	0.54
	DM	0.21	0.83	0.13	0.51	−0.42

repeated measurements can provide more data for better applications of statistical tools. However, this type of analysis can also show some limitations, as in our case, we could not quantify the influence of wind direction due to accumulated uncertainties. Therefore, we could not associate and quantify certain adverse effects with wind direction, though it seems reasonable to assume that direction is a variable that can be of influence.

Looking back at the entire experience gained in this investigation, we can say that gas tracer techniques present limitations in assessing the airflow rate for in-field or in-field-like experiments due to the rather complex experimental set-up, at least compared to other methods as the VTM. We also need to consider that they have shown a relatively high uncertainty, not far better than the simpler methods may offer. Using CO_2 as a tracer gas is a more environmentally friendly solution than other tracer gas, yet it is not free from impacting the environment. Alternative promising techniques suitable for continuous measurements, such as methods based on the orifice plate or ultrasonic measurements, could be further developed and compared to tracer gas methods in future studies to expand the analysis of the reliability of the different techniques for different measurement ranges.

Though one of the original goals of the investigation was to define clear best-practice procedures and guidelines for this type of experimental activity, we need to consider that this goal could not be fully developed based on the experiments we could carry out at this stage, as we realized that we would have needed to develop a more comprehensive experimental campaign that included DSFs of different dimensions, ventilation modes, weather conditions, and further variables that are outside the possibilities that we currently have. We nevertheless hope that our reflections on these techniques and the sharing of our experience with this particular set of measurements will help other researchers in carrying out their experiments and that, cumulatively, a more robust set of guidelines for tracer gas techniques applied to ventilated facades can be developed in the long run.

5. Conclusion

The outcomes of this study, which aimed at investigating how gas tracer techniques can be performed for in-field or in-field-like experiments and at assessing their performance in such context against a reference method (VTM), can be summarised according to the following points: dosing of the tracer gas, points of injection of the tracer gas, points for a sampling of the tracer gas, the overall performance of the techniques, and their applicabilities.

CO_2 dosing - In order to prevent unrealistic airflow estimation, CIM requires that the average CO_2 concentration in the cavity is several times higher than the background level (five or more times) with a reasonable upper limit of 5000 ppm that limits modification of air mixture and its dynamics. For the same reason, the initial CO_2 concentration in the DM should generally not exceed 10,000 ppm.

Injection points - Using several injection points in the cavity is desirable in both methods. In CIM, the CO_2 sources need to be placed at one height level nearby and above the inlet to allow the longest possible mixing path, whereby attention should be paid to avoid CO_2 'wash-out' effect. Injection points in DM should be distributed along several heights between inlet and outlet in both half-cavities to evenly disperse CO_2 along the airflow path. If a uniform distribution can not be achieved, an additional fan can be installed to mix more thoroughly CO_2 right before the start of decay time measurement while the cavity is still closed.

Sampling points – It is recommended that CO_2 sensors in CIM are placed evenly in the cavity at one height level close to the outlet, assuring that measurements are not influenced by outside air. Sampling points in DM should be distributed uniformly in the cavity volume so one may extract volumetric average values and check the homogeneity of CO_2 distribution.

Performance of the tracer gas techniques – Both techniques showed significant offsets compared to the velocity traverse method (VTM). CIM tends to overestimate the airflow, most likely due to the sudden drops in CO_2 concentration linked to the wind strikes and sudden and sporadic penetration of CO_2-depleted air in the cavity. DM tends to underestimate the airflow, which may arise from slow subsidence of highly concentrated CO_2, causing a longer time of CO_2 extraction. However, CIM showed acceptable agreement with VTM for configuration with higher airflow rates (air velocities over 0.1 ms^{-1}), while DM showed potential to be one of the few methods, if not the only one, available to estimate very low airflow rates.

Applicability of the techniques to in-field measurements - Both techniques have shown considerable limitations regarding airflow rate assessment in a field or in-field-like experiments due to the complex experimental set-up and relatively high uncertainty. For example, DM proved unsuitable for DSF configurations with large airflow rates where a significant volume of CO_2 needs to be injected to achieve a sufficiently long decay time, while CIM showed to be more sensitive to wind influences arising from the equation where the airflow is inversely proportional to the difference in CO_2 concentration. In this context of in-field experiments, statistical tools are essential elements to process data and reach sound conclusions. Repeated measurements are also a suitable strategy to obtain enough data, enabling more robust statistical processing of the collected measurements.

CRediT authorship contribution statement

Aleksandar Jankovic: Writing – original draft, Visualization, Methodology, Investigation, Formal analysis, Data curation, Conceptualization. **Giovanni Gennaro:** Data curation, Investigation, Methodology, Software, Writing – original draft. **Gaurav Chaudhary:** Writing – review & editing, Software, Investigation, Data curation. **Francesco Goia:** Conceptualization, Formal analysis, Funding acquisition, Methodology, Project administration, Resources, Supervision, Writing – review & editing. **Fabio Favoino:** Writing – review & editing, Supervision, Resources, Methodology, Investigation, Conceptualization, Project administration.

Declaration of competing interest

The authors declare that they have no known competing financial interests or personal relationships that could have appeared to influence the work reported in this paper.

Acknowledgments

The experimental activities presented in this paper were carried out within the research project "REsponsive, INtegrated, VENTilated - REINVENT – windows" (research grant no. 262198), supported by the Research Council of Norway and the partners SINTEF, Hydro Extruded Solutions, Politecnico di Torino, and Aalto University. Methods for data processing, data analysis, and overall experimental methods developments contribute to the activities on Characterization and testing of smart building envelope materials, components, and systems within the H2020 project "iclimabuilt - Functional and advanced insulating and energy harvesting/storage materials across climate adaptive building envelopes" (Grant Agreement no. 952886).

We would like to thank the two anonymous reviewers for the positive cooperation during the peer-review process and their valuable comments that helped us improving the quality of the manuscript.

References

[1] A.S. Eugenia Gasparri, Arianna Brambilla, Gabriele Lobaccaro, Francesco Goia, Annalisa Andaloro (Eds.), Rethinking Building Skins – Transformative Technologies and Research Trajectories, Woodhead Publishing Series in Civil and Structural Engineering, 2021.

[2] R.C.G.M. Loonen, M. Trčka, D. Cóstola, J.L.M. Hensen, Climate adaptive building shells: state-of-the-art and future challenges, Renew. Sustain. Energy Rev. 25 (2013) 483–493.

[3] M. Perino, V. Serra, Switching from static to adaptable and dynamic building envelopes: a paradigm shift for the energy efficiency in buildings, J. Facade Des. Eng. 3 (2015) 143–163.

[4] E. Taveres-Cachat, S. Grynning, J. Thomsen, S. Selkowitz, Responsive building envelope concepts in zero emission neighborhoods and smart cities - a roadmap to implementation, Build. Environ. 149 (2019) 446–457.

[5] W. Streicher, et al., On the typology, costs, energy performance, environmental quality and operational characteristics of double skin facades in European buildings, Adv. Build. Energy Res. 1 (2007) 1–28.

[6] E. Oesterle, R.-D. Lieb, M. Lutz, W. Heusler, Double-skin facades : *integrated planning*, München : Prestel (2001).

[7] M.M.S. Ahmed, A.K. Abel-Rahman, A.H.H. Ali, M. Suzuki, Double skin façade: the state of art on building energy efficiency, J. Clean. Energy. Technol. 4 (1) (2015) 84–89.

[8] F. Kuznik, T. Catalina, L. Gauzere, M. Woloszyn, J.J. Roux, Numerical modelling of combined heat transfers in a double skin faade - full-scale laboratory experiment validation, Appl. Therm. Eng. 31 (14–15) (2011) 3043–3054.

[9] M.A. Shameri, M.A. Alghoul, K. Sopian, M.F.M. Zain, O. Elayeb, Perspectives of double skin façade systems in buildings and energy saving, Renew. Sustain. Energy Rev. 15 (3) (2011) 1468–1475.

[10] A. Ghaffarianhoseini, A. Ghaffarianhoseini, U. Berardi, J. Tookey, D.H.W. Li, S. Kariminia, Exploring the advantages and challenges of double-skin façades (DSFs), Renew. Sustain. Energy Rev. 60 (2016) 1052–1065.

[11] M.H. Oh, K.H. Lee, J.H. Yoon, Automated control strategies of inside slat-type blind considering visual comfort and building energy performance, Energy Build. 55 (Dec. 2012) 728–737.

[12] M.G. Gomes, A.J. Santos, A.M. Rodrigues, Solar and visible optical properties of glazing systems with Venetian blinds: numerical, experimental and blind control study, Build. Environ. 71 (2014) 47–59. Complete.

[13] C.-S. Park, G. Augenbroe, N. Sadegh, M. Thitisawat, T. Messadi, Real-time optimization of a double-skin façade based on lumped modeling and occupant preference, Build. Environ. 39 (8) (2004) 939–948.

[14] S.-H. Yoon, C.-S. Park, G. Augenbroe, On-line parameter estimation and optimal control strategy of a double-skin system, Build. Environ. 46 (5) (2011) 1141–1150.

[15] V. Gavan, M. Woloszyn, F. Kuznik, J.-J. Roux, Experimental study of a mechanically ventilated double-skin façade with Venetian sun-shading device: a full-scale investigation in controlled environment, Sol. Energy 84 (2) (2010) 183–195.

[16] A. Zöllner, E.R.F. Winter, R. Viskanta, Experimental studies of combined heat transfer in turbulent mixed convection fluid flows in double-skin-façades, Int. J. Heat Mass Tran. 45 (22) (2002) 4401–4408.

[17] H. Manz, A. Schaelin, H. Simmler, Airflow patterns and thermal behavior of mechanically ventilated glass double facades, Build. Environ. 39 (9) (2004) 1023–1033.

[18] D. Saelens, Energy Performance Assessment of Single Storey Multiple-Skin Facades, Catholic University of Leuven, 2011.

[19] T. Inan, T. Başaran, M.A. Ezan, Experimental and numerical investigation of natural convection in a double skin facade, Appl. Therm. Eng. 106 (2016) 1225–1235.

[20] T. Inan, T. Basaran, A. Erek, Experimental and numerical investigation of forced convection in a double skin façade, Energies 10 (2017) 9.

[21] S. Hassanli, G. Hu, K.C.S. Kwok, D.F. Fletcher, Utilizing cavity flow within double skin façade for wind energy harvesting in buildings, J. Wind Eng. Ind. Aerod. 167 (2017) 114–127.

[22] L. Mei, D. Loveday, D. Infield, V. Hanby, M. Cook, Y. Ji, M. Holmes, J. Bates, The influence of blinds on temperatures and air flows within ventilated double-skin facades, Proc. Clima 2007 WellBeing Indoors (2007). http://usir.salford.ac.uk/id/eprint/15870/1/Clima_2007_B02E1606.pdf.

[23] T. Inan, T. Basaran, Experimental and numerical investigation of forced convection in a double skin façade by using nodal network approach for Istanbul. Sol, Energy 183 (2019) 441–452.

[24] T. Başaran, T. İnan, Experimental investigation of the pressure loss through a double skin facade by using perforated plates, Energy Build. 133 (2016) 628–639.

[25] G. Gennaro, F. Fabio, F. Goia, G. De Michele, M. Perino, Calibration of DSF model for real-time control, in: Journal of Physics: Conference Series, 2069, IBPC, 2021, 012027.

[26] O. Kalyanova, Double-skin Facade: Modelling and Experimental Investigations of Thermal Performance, 2008.

[27] International Organization for Standardization, EN 16211:2015 Ventilation for Buildings - Measurement of Air Flows on Site - Methods, 2015.

[28] International Organization for Standardization, ISO 12599-2012 Ventilation for Buildings - Test Procedures and Measurement Methods to Hand over Air Conditioning and Ventilation Systems, 2012.

[29] International Organization for Standardization, ISO 16956:2015 Thermal Performance in the Built Environment — Determination of Air Flow Rate in Building Applications by Field Measuring Methods, 2015.

[30] S.B. Riffat, Comparison of tracer-gas techniques for measuring air flow in a duct, J. Inst. Energy 63 (1990) 18–21.

[31] International Organization for Standardization, ISO 12569: 2017 Thermal Performance of Buildings and Materials - Determination of Specific Airflowrate in Buildings - Tracer Gas Dilution Method, 2017.

[32] D. Laussmann, in: D.H.E.N. Mazzeo (Ed.), Air Change Measurements Using Tracer Gases: Methods and Results. Significance of Air Change for Indoor Air Quality, IntechOpen, Rijeka, 2011, p. 14.

[33] S.P. Corgnati, M. Perino, V. Serra, Experimental assessment of the performance of an active transparent façade during actual operating conditions, Sol. Energy 81 (8) (2007) 993–1013.

[34] L.C.O. Souza, H.A. Souza, E.F. Rodrigues, Experimental and numerical analysis of a naturally ventilated double-skin façade, Energy Build. 165 (2018) 328–339.

[35] E. Giancola, et al., Possibilities and challenges of different experimental techniques for airflow characterisation in the air cavities of façades, J. Facade Des. Eng. 6 (3) (Aug. 2018), https://doi.org/10.7480/jfde.2018.3.2470. Spec. Issue FAÇADE 2018 – Adapt.

[36] N. Safer, Modélisation des façades de type double-peau équipées de protections solaires : approches multi-échelles, L'Institut National des Sciences Appliquées de Lyon (2006).

[37] O. Kalyanova, P. Heiselberg, Experimental Set-Up and Full-Scale Measurements in the 'Cube, Aalborg University, 2008. Aalborg.

[38] R.L. Jensen, O. Kalyanova, C.-E. Hyldgård, On the use of hot-sphere anemometers in a highly transient flow in a double-skin façade, in: Proceedings of Roomvent 2007: Helsinki 13-15 June 2007, FINVAC ry, 2007.

[39] K.J. King, Turbulent Natural Convection in Rectangular Air Cavities, Queen Mary University of London, 1989.

[40] M. Bhamjee, A. Nurick, D.M. Madyira, An experimentally validated mathematical and CFD model of a supply air window: forced and natural flow, Energy Build. 57 (2013) 289–301.

[41] O. Kalyanova, R.L. Jensen, P. Heiselberg, Measurement of air flow rate in a naturally ventilated double skin façade, in: Proceedings of Roomvent 2007: Helsinki 13-15 June 2007, FINVAC ry, 2007.

[42] G. Myhre, D. Shindell, J. Pongratz, Anthropogenic and Natural Radiative Forcing. Climate Change 2013: The Physical Science Basis. Contribution of Working Group I to the Fifth Assessment Report of the Intergovernmental Panel on Climate Change [Stocker, T.F., D. Qin, G.-K. Plattner, M. Tignor, S.K. Allen, J. Boschung, A. Nauels, Y. Xia, V. Bex and P.M. Midgley (eds.)]., Cambridge University Press, Cambridge, United Kingdom and New York, NY, USA, 2014.

[43] D. Etheridge, M. Sandberg, Building Ventilation: Theory and Measurement, Wiley, 1997.

[44] H. Poirazis, Double skin façades for office buildings, Report EBD (2004).

[45] G. Remion, B. Moujalled, M. El Mankibi, Review of tracer gas-based methods for the characterization of natural ventilation performance: comparative analysis of their accuracy, Build. Environ. 160 (2019), 106180.

[46] N. Nikolopoulos, A. Nikolopoulos, T.S. Larsen, K.-S.P. Nikas, Experimental and numerical investigation of the tracer gas methodology in the case of a naturally cross-ventilated building, Build. Environ. 56 (2012) 379–388.

[47] F. Marques da Silva, M.G. Gomes, A.M. Rodrigues, Measuring and estimating airflow in naturally ventilated double skin facades, Build. Environ. 87 (2015) 292–301.

[48] A. Jankovic, F. Goia, Impact of double skin facade constructional features on heat transfer and fluid dynamic behaviour, Build. Environ. 196 (2021), 107796.

[49] V. Serra, F. Zanghirella, M. Perino, Experimental evaluation of a climate façade: energy efficiency and thermal comfort performance, Energy Build. 42 (1) (2010) 50–62.

[50] R.R. Rothfus, D.H. Archer, I.C. Klimas, K.G. Sikchi, Simplified flow calculations for tubes and parallel plates, AIChE J. 3 (2) (1957) 208–212.

[51] H.C. Lim, M. Ohba, Interference effects of three consecutive wall-mounted cubes placed in deep turbulent boundary layer, J. Fluid Mech. 756 (2014) 165–190.

[52] J. Zheng, Q. Tao, L. Li, "Wind pressure coefficient on a multi-storey building with external shading louvers, Appl. Sci. 10 (2020) 3. https://doi.org/10.3390/app10031128, 1128.

[53] R. Jin, et al., "Numerical investigation of wind-driven natural ventilation performance in a multi-storey hospital by coupling indoor and outdoor airflow, Indoor Built Environ. 25 (8) (2015) 1226–1247.

[54] A. Jankovic, M.S. Siddiqui, F. Goia, Laboratory testbed and methods for flexible characterization of thermal and fluid dynamic behaviour of double skin facades, Building and Environment 210 (2022), 108700. In press, https://doi.org/10.1016/j.buildenv.2021.108700.